used in treatment assessment. We study these relationships in three functional imaging techniques in head and neck cancer patients.

Materials and Methods: We analyse data from a patient included in the ARTFIBio project [1], which includes functional imaging for treatment planning and along the treatment. The three different imaging modalities are: Apparent Diffusion Coefficient (ADC) maps and Dynamic Contrast Enhanced MRI (DCEMRI), pre-treatment and at 13th fraction, and 18F-FDG PET/CT, only pre-treatment. We evaluate them as biological markers. Thus, vascularization measured by DCE-MRI parameters (k_{trans}) can determine tumour hypoxia, ADC maps can evaluate tumour cell density, and glucose consumption from FDG PET/CT can assess the Warburg effect enhancement. Glucose metabolism is related to hypoxia (Pasteur effect) and tumour cell density, although it includes additional information about malignancy (Warburg effect). The product of ADC, SUV and k_{trans} can be useful for determine the Warburg effect enhancement, because ADC less ADC_{min} is inversely proportional to tumour cell density.

Results:

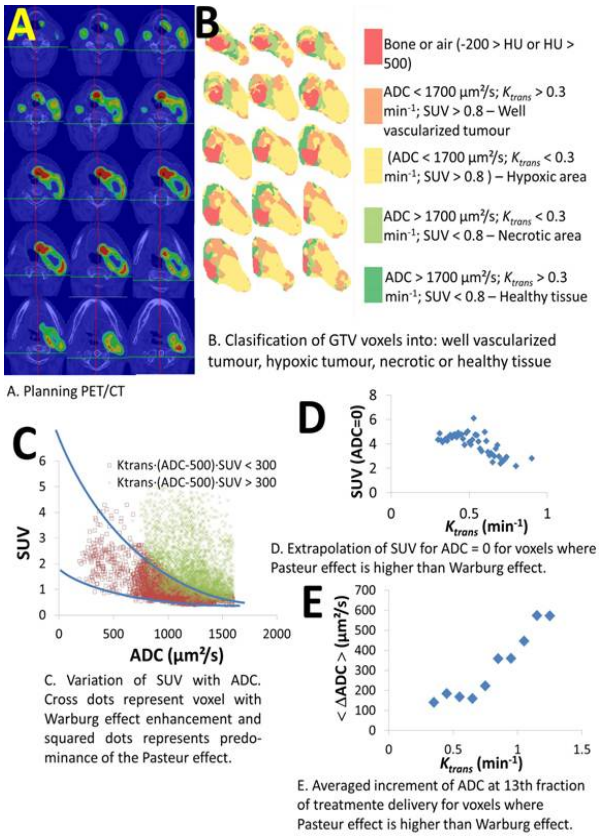

Fig. 1A shows the planning PET/CT, and GTV voxels has been classified (Fig. 1B) as: well or badly vascularized tumour, necrotic areas and healthy tissue. We have analysed the relationship between SUV, ADC and k_{trans} (Fig. 1C). If we take into account only those voxels where the Pasteur effect is more relevant than the Warburg effect, a decreasing function (Fig. D) is obtained for the maximum FDG consumption varying the vascularization, as expected if k_{trans} is a marker of oxygen level, and a sigmoid curve is showed in Fig. E for the averaged increment of ADC between the pre-treatment study and the study performed along the treatment. This last curve reflects a related behaviour to the oxygen enhance ratio used in rabiobiological models, suggesting that k_{trans} is a hypoxia marker for head and neck cancer, and ADC is related inversely to tumour cell density.

Conclusions: A dataset for achieving the biologically guided radiotherapy must include a tumour density study and a hypoxia marker. Considering the datasets used in the ARTFIBio project [1], k_{trans} from DCEMRI can be used for indirectly measuring oxygen levels in head and neck cancer, tumour cell density can be evaluated by ADC maps, and a relative measure of the malignancy (Warburg effect enhancement) can be deduced from the link of the three datasets.

Funded by FIS PI11/02035 grant and by FP7/REGPOT-2012-2013.1 (grant agreement n° 316265, BIOCAPS).

[1] M. Mera Iglesias, D. Aramburu, JL del Olmo, et al., 'Multimodality Functional Imaging in Radiation Therapy Planning: Relationships between Dynamic Contrast-Enhanced MRI, Diffusion-Weighted MRI, and 18F-FDG PET,' Computational and Mathematical Methods in Medicine, Article ID 103843, in press.

PO-0953

Quantitative diffusion-weighted MRI of rectal cancer is strongly influenced by the choice of b-values

M. Bornstein[1], A. Negård[2], S.H. Holmedal[2], A.S. Borthne[2], A.H. Ree[1], K. Røe[1]

[1]*Akershus University Hospital, Department of Oncology, Oslo, Norway*

[2]*Akershus University Hospital, Department of Radiology, Oslo, Norway*

Purpose/Objective: In rectal cancer, diffusion-weighted (DW) MRI is increasingly being employed in assessment of local tumor extension as well as in prediction and monitoring of chemoradiotherapy response. The apparent diffusion coefficient (ADC) can be calculated from DWI acquired with at least two degrees of diffusion-weighting, i.e., b-values. However, in rectal cancer no consensus on the choice of optimal b-values for ADC calculation exists, which also limits the ability to compare ADCs between patients and institutions. To calculate ADCs the most widely used approach is the simplified monoexponential model, whereas a more general approach is the biexponential model accounting for contributions from blood perfusion to the diffusion signal. The purpose of this study was to examine how the choice of b-values in the monoexponential model affects the resulting ADCs and to compare these to the ADC calculated using the biexponential model.

Materials and Methods: As part of primary staging, DW MRI using six b-values (b = 0, 25, 50, 100, 500, and 1000 s/mm^2) were prospectively acquired from 10 rectal cancer patients on a 1.5T Philips Achieva MRI scanner. Two experienced readers independently contoured whole-tumor regions-of-interest (ROIs) by means of free-hand delineations, before tumor ADCs were calculated from 11 different combinations of b-values using the monoexponential model. The ADC from the biexponential model incorporating all b-values was used as the reference. The Wilcoxon matched-pairs signed rank test was used to assess differences in ADCs. Intraclass correlation coefficients (ICC) and Bland-Altman plots were used to evaluate interobserver variability.

Results: The whole-tumor ROI interobserver agreement was excellent (ICC = 0.97). The study uncovered significant variability in monoexponentially calculated tumor ADCs when different combinations of b-values were used (Figure 1). When calculating ADCs using all six b-values the monoexponential model overestimated the median tumor ADC by 85% (P = 0.001) compared to the reference ADC from the biexponential model. The ADCs were significantly reduced when excluding the low b-values (0, 50 and 100 s/mm^2) in the calculation. The b = 0 s/mm^2 is commonly included in the ADC calculation; this study shows that its inclusion results in a substantial overestimation. The combination of b = 500 and 1000 s/mm^2 resulted in a deviation of only 19% compared to the reference ADC.

Figure 1. Influence of b-values on tumor ADC

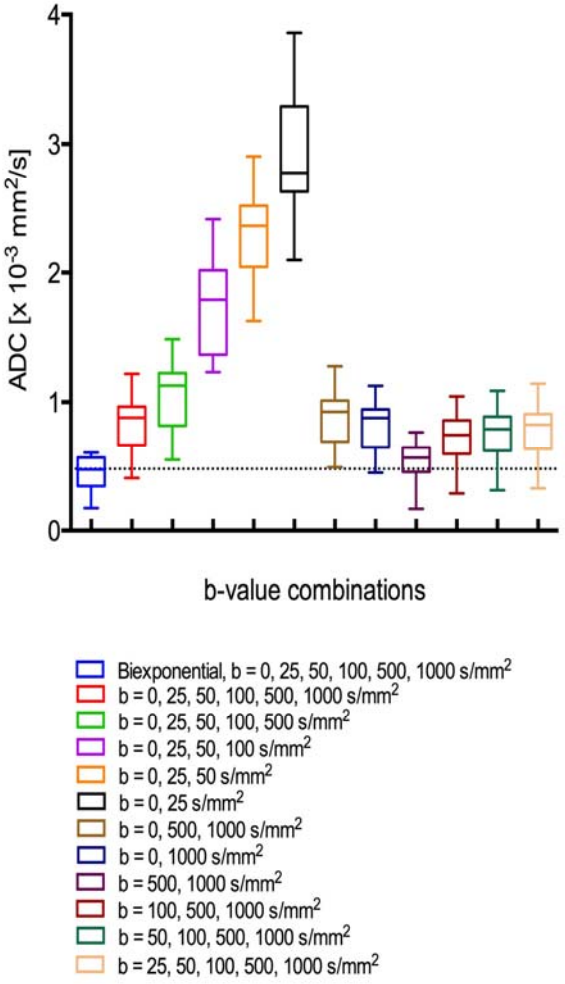

Conclusions: In rectal cancer the tumor ADC calculated using the monoexponential model is strongly influenced by the choice of b-values. By eliminating the contribution of perfusion (b-values ≤ 100 s/mm^2) the uncertainty in the ADC calculation is significantly reduced. Quantitative comparison of ADCs between patients and institutions cannot be performed if the ADC is calculated using DW images with different b-values.

PO-0954

Evaluation of specific and general-purpose atlases for automatic segmentation in breast cancer radiotherapy

D. Ciardo[1], M.A. Gerardi[2], S. Vigorito[3], R. Ricotti[2], M.C. Leonardi[2], A. Morra[2], V. Dell'Acqua[2], F.J. Diaz[4], F. Cattani[3], G. Baroni[5], B.A. Jereczek-Fossa[2], R. Orecchia[6]

[1]*European Institute of Oncology, Division of Radiotherapy, Milan, Italy*

[2]*European Institute of Oncology and University of Milan, Division of Radiotherapy, Milan, Italy*

[3]*European Institute of Oncology, Unit of Medical Physics, Milan, Italy*

[4]*Mevaterapia, Medical Radiation Oncology, Buenos Aires, Argentina*

[5]*Politecnico di Milano, Dipartimento di Elettronica Informazione e Bioingegneria, Milan, Italy*

[6]*European Institute of Oncology and University of Milan and Centro Nazionale Adroterapia Oncologica (CNAO), Division of Radiotherapy, Milan, Italy*

Purpose/Objective: To evaluate atlas-based autosegmentation of target and organs at risk (OARs) for breast cancer patients by comparing purpose-specific and generic atlases.

Materials and Methods: Atlas elaboration and autosegmentation were performed using MIMvista. Two hundred CT scans of post-operative breast cancer patients were used to create atlases. For treatment planning, about 15 structures were manually segmented for each patient. A generic atlas was obtained using the whole cohort of patients. Nine sub-atlases were obtained combining information about surgical procedure (mastectomy or conservative surgery), side of the tumor (left/right) and thoracic circumference (small/medium/large). Each sub-atlas was composed of about 20 patients (range 14-29). Forty-seven previously contoured CT scans not included in the atlases were selected as test-set and used to compare automatic and manual segmentation. Characteristics of patients constituting the sub-atlases and the test-set is shown in table. Automatically segmented structure sets were obtained from generic atlas (GEN), specific atlas (SPEC, considering the size of the thoracic circumference and the side of the tumor), specific atlas with keywords (S-KEY, related to the size of contralateral breast, the presence of breast implant and expander). Moreover, the performance of the simultaneous truth and performance level estimation (STAPLE) algorithm applied to the best 3 matching subjects of specific (S-STAPLE) and generic (G-STAPLE) atlases were also evaluated. For each test-CT scan, five automatically segmented structure sets were therefore obtained, each composed of 10-12 OARs. A quantitative evaluation was performed computing center of mass distance (CMD), Dice similarity coefficient (DSC) and Hausdorff distance (HD) between corresponding automatically and manually segmented structures.